JOURNAL OF GEOPHYSICAL RESEARCH, VOL. 90, NO. C5, PAGES 9159–9167, SEPTEMBER 20, 1985

Calibration and Verification of a Dissipation Model for Random Breaking Waves

J. A. BATTJES

Delft University of Technology, The Netherlands

M. J. F. STIVE

Delft Hydraulics Laboratory, The Netherlands

A model describing the average rate of energy dissipation in random waves breaking in shallow water, published previously by Battjes and Janssen (1978), has been applied to an extensive set of data for the purposes of calibration and verification. Both laboratory and field data were used, obtained on beaches with a more or less plane slope as well as on barred beaches, and for a wide range of wave conditions. Optimal values have been estimated for an adjustable breaking wave height-coefficient in the model; these appear to vary slightly but systematicaly with the incident wave steepness, in a range that is physically realistic. A parameterization of this dependence allows the use of the model for prediction. Applied to the present data set, the correlation coefficient between measured and predicted rms wave heights is 0.98, with an rms normalized error of 6% and a bias that does not differ significantly from zero.

1. INTRODUCTION

The principal physical process in the surf zone is the dissipation of the energy of incident wind waves and swell, due to wave breaking. Because of the randomness of wind-generated waves, the occurrence of breaking at a fixed location is itself a random process. Realistic models for the prediction of the onshore variation of wave energy and radiation stress should take this randomness into account.

Early models for random breaking waves [*Collins*, 1970; *Battjes*, 1972; *Goda*, 1975] express the local mean wave energy directly in terms of the incident wave parameters and the local depth, without considering energy sources or sinks explicitly. These models are physically not well founded.

Battjes and Janssen [1978], hereafter referred to as BJ, presented an alternative approach, in which the local mean rate of energy dissipation is modeled, based on that occurring in a bore and on the local probability of wave breaking. The result is used as a sink in the energy balance, which is subsequently integrated to obtain the wave energy as a function of onshore distance. The advantages of this approach compared with the earlier models are that other sources or sinks than those due to breaking can be accommodated without difficulty, and that the depth need not be monotonically decreasing in the propagation direction. A few laboratory experiments performed by BJ, including cases with a bar-trough profile, indicated a very promising degree of agreement.

Thornton and Guza [1983] have presented a refinement of BJ's model, which however has negligible consequences for the predicted rms variation. They also made a comparison between calculated and measured rms wave heights, using field data of low swell incident on a gently sloping, almost plane beach. Good agreement was found, with an rms relative error of about 9%.

The range of bottom profiles and incident wave parameters in the measurements referred to above is too restricted to allow a systematic investigation of the model performance and of the optimum values of the adjustable parameters. It was therefore decided to carry out an extensive calibration and verification of the model. The purpose of this paper is to present the results of this investigation.

Paper number 5C0154.
0148-0227/85/005C-0154$05.00

2. SUMMARY OF BATTJES AND JANSSEN'S MODEL

In BJ's estimation of the time-averaged rate of dissipation of wave energy per unit area due to breaking ($\bar{D}$), two aspects can be distinguished: the rate of energy dissipation in a single breaking wave, and the probability of occurrence of breaking waves of given height.

Following *Stoker* [1957], *LeMéhauté* [1962], and others, the energy dissipation in a breaking wave is modeled after that in a bore connecting two regions of uniform flow. This results in the following order-of-magnitude relation for the rate of energy dissipation per unit horizontal area (D):

$$D \sim \tfrac{1}{4} f \rho g H_b^2 \tag{1}$$

in which f is the wave frequency, ρ the water's mass density, g the gravitational acceleration, and H_b the (trough-to-crest) height of the breaking wave.

For application to random waves, the expected value of D (written as $\bar{D}$) must be estimated, taking into account the randomness of the waves and the fact that not all the waves passing the point considered are breaking. The frequency at the peak of the energy spectrum of the incident waves is used for the frequency (f) in (1), whereas the mean square of the random variable H_b is equated to the square of the nominal, depth-limited height of periodic waves (H_m) in water of the local mean depth (h). BJ use a Miche-type expression for H_m, adapted through the inclusion of a parameter γ to account for influences of bottom slope and incident wave steepness:

$$H_m = 0.88 k_p^{-1} \tanh(\gamma k_p h / 0.88) \tag{2}$$

The wave number k_p is calculated on the basis of the linear-theory dispersion equation for gravity waves with frequency f_p.

To determine the local fraction of breaking waves (Q), BJ assume that the cumulative probability distribution of all

wave heights (breaking or nonbreaking) is of the Rayleigh type, cut off discontinuously at $H = H_m$. This was shown to imply the following relation between Q and H_{rms}/H_m, in which H_{rms} is the rms of all wave heights:

$$\frac{1-Q}{-\ln Q} = \left(\frac{H_{rms}}{H_m}\right)^2 \tag{3}$$

Substituting the approximations mentioned above in the averaged relation (1), and writing the order-of-magnitude relation in the form of an equation, gives

$$\bar{D} = \tfrac{1}{4}\alpha Q f_p \rho g {H_m}^2 \tag{4}$$

in which α is a coefficient that is expected to be of order 1. It is pointed out that $\bar{D}$ depends on H_{rms} through Q.

To close the model, $\bar{D}$ is used as a sink in the wave energy balance, which in its most reduced form (statistically steady, uniform alongshore, no other sources or sinks than $\bar{D}$) can be written as

$$\frac{\partial P_x}{\partial x} + \bar{D} = 0 \tag{5}$$

P_x is the onshore energy flux per unit width, approximated as Ec_g, in which $E = \frac{1}{8}\rho g {H_{rms}}^2$ and c_g is the group velocity according to the linear theory for $f = f_p$.

For known depth profile $h(x)$, incident wave values for f_p and H_{rms}, and estimates of the coefficients α and γ, (5) can be integrated numerically to obtain the onshore variation of H_{rms}. In this process, f_p is treated as a constant. Note that the model calculates the local value of the fraction of breaking waves, Q. It is principally through variations of Q that the model reacts to changes in depth.

In the applications given below the mean depth (h) is the sum of the bottom depth below still water level (d) and a wave-induced set-up ($\bar{\eta}$). The latter has been calculated through the simultaneous integration of the energy balance (5) and the mean momentum balance in the form

$$\frac{\partial S_{xx}}{\partial x} + \rho g(d+\bar{\eta})\frac{\partial \bar{\eta}}{\partial x} = 0 \tag{6}$$

[*Longuet-Higgins and Stewart*, 1963]. The radiation stress component S_{xx} has been calculated according to

$$S_{xx} = \left(\frac{1}{2} + \frac{2k_p h}{\sinh 2k_p h}\right)E \tag{7}$$

The prediction of $\bar{\eta}(x)$ allows a further check on the theory, in addition to that of $H_{rms}(x)$.

3. OBSERVATIONS

Empirical data from various sources have been collected for calibration and verification of the theoretical model. These include laboratory and field data obtained for a variety of wave conditions and bottom profiles. The original data of BJ are included also.

All laboratory data used herein have been collected in wave flumes, using mechanically generated random waves. The field sites and conditions were selected so as to have more or less statistically uniform conditions alongshore and normal wave incidence (for the principal propagation direction). Direct wind influence was negligible in all cases considered here, as will be explained further on.

The laboratory bottom profiles include plane slopes and a schematized bar profile in concrete, as well as concave and barred profiles in sand. The collected data are primarily based on small-scale measurements with incident rms wave heights ranging from 0.10 to 0.21 m. One of the data series was obtained in a large-scale wave facility with an incident rms wave height of 1.00 m.

Two field sites on the Dutch coast were used, one on a beach near the city of Egmond with a double bar system, the other on a shoal in the mouth of the Haringvliet estuary (see Figure 1). The Egmond beach measurement series were collected both under moderate conditions with incident rms wave heights up to 1.3 m and under storm conditions with incident rms wave heights up to 2.8 m. The measurements in the Haringvliet estuary were conducted in a line across an elongated shoal, with more or less parallel depth contours over a distance of about 5000 m (see Figure 1). The minimum depth over the shoal is 0.1 m below mean sea level, and about 1.5 m below mean high water Level. Here measurements were collected under a variety of conditions of which a swell series (incident rms wave heights of 0.9 m) and a storm series (incident rms wave heights of 2.4 m) at near-normal incidence were selected for the present study.

Each data series comprised the measurement of the bottom profile, the measurement of the mean water level, rms wave height and peak frequency at an offshore reference point, and the measurement of the rms wave heights at various points in the profile. In some cases the variation of mean water level with distance onshore was measured also. In the field cases, a number of up to six measurement series differing only slightly in incident conditions were combined and averaged to reduce the influence of measurement errors and inaccuracies. The re-

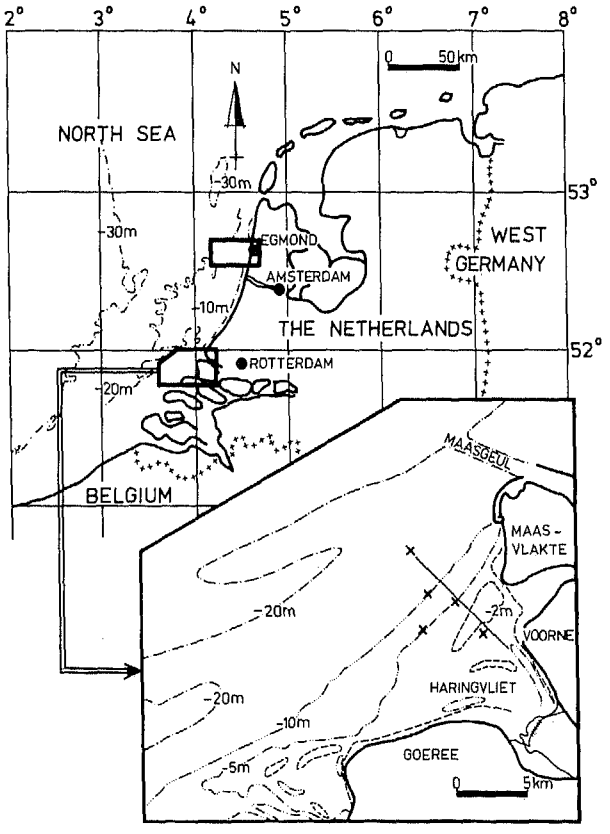

Fig. 1. Situation map showing field sites. Egmond: cases 17 and 18; Haringvliet: cases 19 and 20. Insert: depth contours of Haringvliet site with wave height stations marked.

TABLE 1. Experimental and Environmental Parameters

Serial Number	Source	Profile	h_r, m	H_{rms_r}, m	f_{pr}, Hz	s_0	$\hat{\gamma}$
		Laboratory					
1	*Battjes and Janssen* [1978]	Plane (1:20)	0.705	0.144	0.511	0.026	0.73
2	*Battjes and Janssen* [1978]	Plane (1:20)	0.697	0.122	0.383	0.012	0.60
3	*Battjes and Janssen* [1978]	Plane (1:20)	0.701	0.143	0.435	0.018	0.70
4	*Battjes and Janssen* [1978]	Schematized bar-trough	0.703	0.137	0.450	0.019	0.72
5	*Battjes and Janssen* [1978]	Schematized bar-trough	0.645	0.121	0.443	0.016	0.69
6	*Battjes and Janssen* [1978]	Schematized bar-trough	0.763	0.104	0.467	0.016	0.70
7	*Battjes and Janssen* [1978]	Schematized bar-trough	0.732	0.118	0.481	0.019	0.70
8	*Battjes and Janssen* [1978]	Schematized bar-trough	0.616	0.143	0.498	0.024	0.72
9	*Stive* [1985]	Plane (1:40)	0.700	0.138	0.341	0.010	0.62
10	*Stive* [1985]	Plane (1:40)	0.700	0.136	0.633	0.038	0.81
11	*Stive* [1985]	Plane (1:40)	4.19	1.00	0.185	0.023	0.82
12	*Van Overeem* [1983]	Concave	0.800	0.211	0.392	0.022	0.73
13	*Van Overeem* [1983]	Concave	0.800	0.096	0.568	0.022	0.80
14	*Van Overeem* [1983]	Concave	0.800	0.132	0.559	0.029	0.80
15	*Van Overeem* [1983]	Bar-trough	0.800	0.132	0.557	0.029	0.83
16	*Van Overeem* [1983]	Bar-trough	0.800	0.212	0.393	0.022	0.75
		Field					
17	*Derks and Stive* [1984]	Bar-trough	10.80	1.29	0.157	0.022	0.67
18	*Dirks and Stive* [1984]	Bar-trough	15.65	2.78	0.115	0.026	0.73
19	*Dingemans* [1983]	Bar	16.40	0.94	0.143	0.013	0.70
20	*Dingemans* [1983]	Bar	11.10	2.43	0.128	0.028	0.82

Numbers 1–10, concrete beach; numbers 11–20, sand beach.

sults are given in terms of an average value and a standard deviation.

In all small-scale laboratory measurements, surface elevations were measured by means of parallel-wire conductivity wave gages. Although aeration influences the response of the gages, the air content in the breaking waves is estimated low enough to cause only negligible deviations. On the concrete beaches, mean bottom pressures were measured by a piezometric system; this consisted of small taps mounted flush with the bottom, connected by tubes to stilling wells, in which the water level was read by point gages.

In the large-scale laboratory wave experiment, surface elevations were measured with a wave surface follower. The instrument consists of a vertical gage with a conductivity sensor at the bottom tip. The gage moves vertically so as to maintain a constant immersion depth of the sensor, thus registering the time variation of the surface. In order to increase the response in case of steep wave fronts, a similar small horizontal gage was fixed on the vertical gage facing the incoming waves. The mean bottom pressures were measured by an alternative piezometric system, consisting of narrow plastic tubes fixed to the flume walls with their open ends close to the sand bottom; the tubes were connected to transparant stilling wells in which the water level was read by eye.

In the field measurements at Egmond beach, surface elevations were measured by wave buoys offshore and by resistance wire gages nearshore. The possibility of leveling of the gages allowed the measurement of mean water level variations in some cases. In the field measurements in the Haringvliet estuary, wave buoys were used mainly. Both the buoys and the gages can give problems in situations with considerable breaking activity. At the occurrence of steep wave fronts, the buoys occasionally capsize, and the gage response contains spurious peaks following a too rapid rise of surface elevation. Both phenomena are easily recognized in the registration. Those segments on the registration where capsizing occurred were eliminated, whereas the spurious response peaks of the gages were removed by filtering.

As a standard procedure, the surface elevation signals were analyzed to estimate the variance σ^2 and its spectral distribution. The measured variances were used to calculate H_{rms} according to

$$H_{rms} = 8^{1/2}\sigma \tag{8}$$

This relation can be derived on the assumption that the surface elevation is a narrow-band Gaussian process. Although this assumption is not justified inside the surf zone, the result (8) has nevertheless been found in good agreement with observations [*Thornton and Guza*, 1983].

A summary of the independent parameters is given in Table 1. Column 1 gives the serial number used herein. Columns 4, 5, and 6 list the values of h, H_{rms} and f_p at the offshore reference point (indicated with the subscript r). The wave heights measured at the (finite-depth) reference point (H_{rms_r}) have been converted to equivalent deep-water wave heights (H_{rms_0}) using linear shoaling theory for periodic waves with frequency f_p, i.e., $H_{rms_0} = H_{rms_r}\ (c_{g_r}/c_{g_0})^{1/2}$. Values of the corresponding deep-water steepness $s_0 \equiv H_{rms_0}/L_{0p}$ are listed in column 7 of Table 1, in which $L_{0p} = g/(2\pi f_p^2)$. The meaning of the parameter $\hat{\gamma}$, listed in column 8, is explained below.

4. MODEL CALIBRATION

The energy balance (5) contains no sources or sinks of energy other than that due to breaking. The possible importance of dissipation in the bottom boundary layer, and that of input of energy by wind (in the field), was investigated by integrating the energy balance with and without terms representing these additional effects. In the propagation intervals considered here, their influence on the resulting H_{rms} variation was negligible compared to that of the depth-controlled wave breaking. For simplicity of presentation, they will not be further considered in this paper.

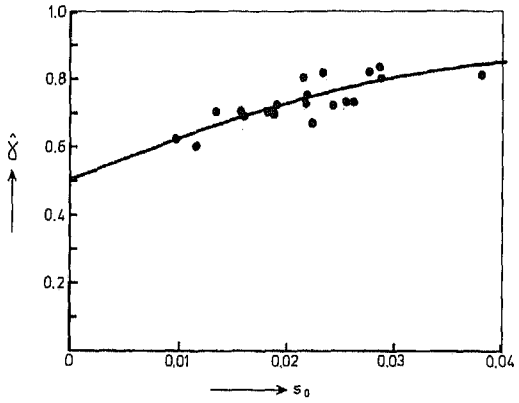

Fig. 2. Estimated values of breaker height coefficient $\hat{\gamma}$ versus deep-water steepness s_0. Data points: optimal value per case. Solid curve: parameterization given by (9).

4.1. *Coefficient Estimation*

The energy balance (5) and the momentum balance (6) have been numerically integrated with respect to the onshore distance (x) for each case listed in Table 1, using the given bottom profile, the reference values of H_{rms} and $\bar{\eta}$, which were taken as initial values in the integration, the reference value of f_p, and chosen values of (α, γ). The peak frequency f_p and the coefficients (α, γ) were kept constant with respect to x. In the vicinity of the mean waterline on the beach, where $h \to 0$ and $Q \to 1$, the model reached saturation; shoreward of the point where this situation is first encountered in the numerical integration, the H_{rms} values were set equal to H_m, i.e., their limiting value for $Q = 1$.

Each integration gives two functions $\bar{\eta}(x)$ and $H_{rms}(x)$ shoreward of the reference point, which can be compared with the measurements. Repeating the integration for several choices of (α, γ), optimal values of these coefficients can be estimated, such that a maximum agreement is obtained between computed and measured values. Actually, this model calibration has been based on a comparison of H_{rms} values only, since the mean water level measurements were available in only a few cases. The agreement between computed and measured values was maximized visually for each of the 20 cases. In this process most weight was given to H_{rms} values in the area of high energy dissipation (this occurred for H_{rms} values which were about half of their initial value).

The coefficients α and γ control the level of energy dissipation in a breaker, and the fraction of breaking waves, respectively. Formally, they can be varied independently of each

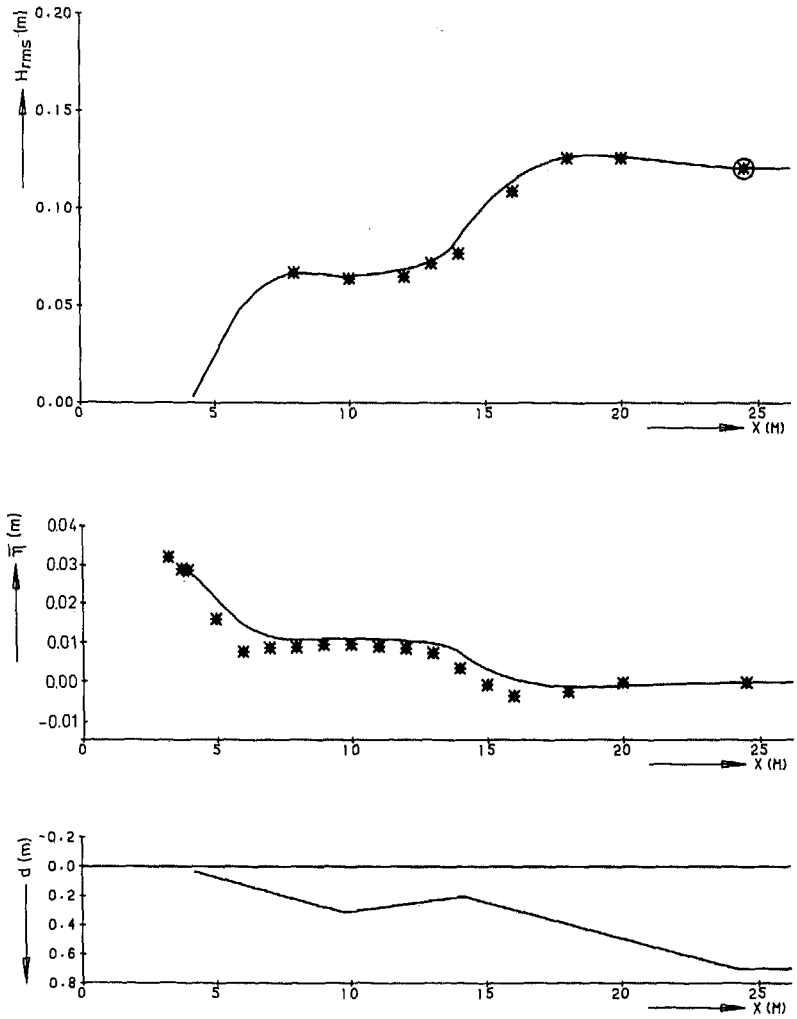

Fig. 3. Results for case 5 (laboratory); profiles of bottom elevation below MWL_r (d), mean water level above MWL_r ($\bar{\eta}$), and rms wave height (H_{rms}) versus distance normal to shore (x). Data points: measured values with offshore reference value encircled. Solid curves: computed values of $\bar{\eta}$ and H_{rms}, based on parameterization of γ given by (9).

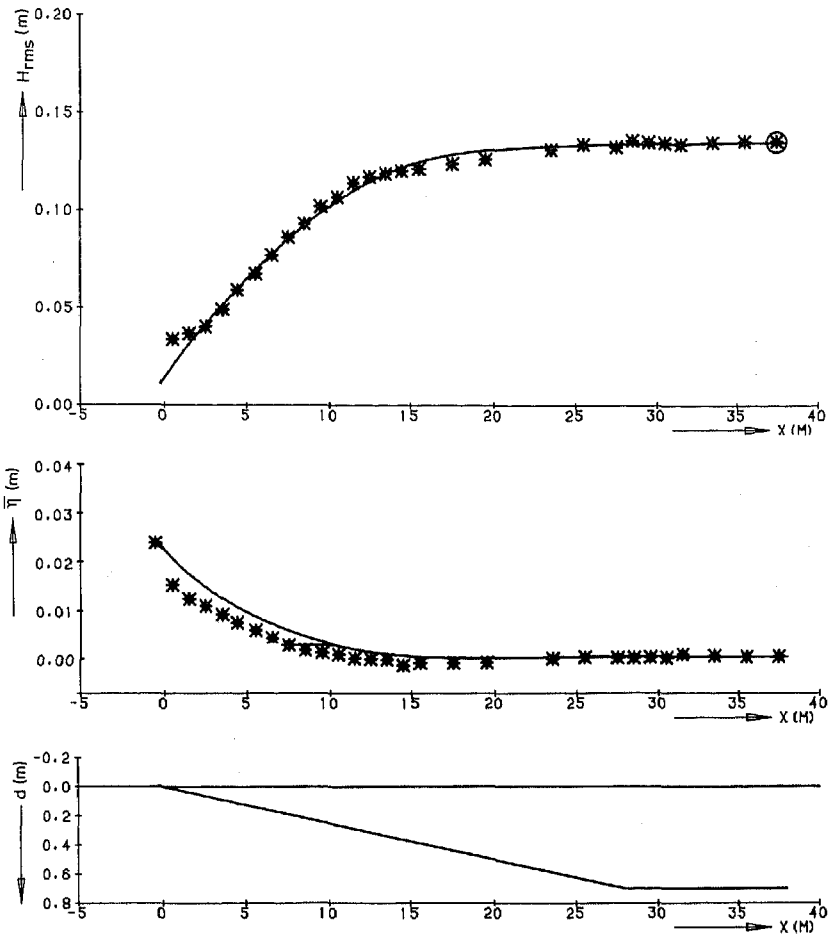

Fig. 4. Results for case 10 (laboratory). For legend, see Figure 3.

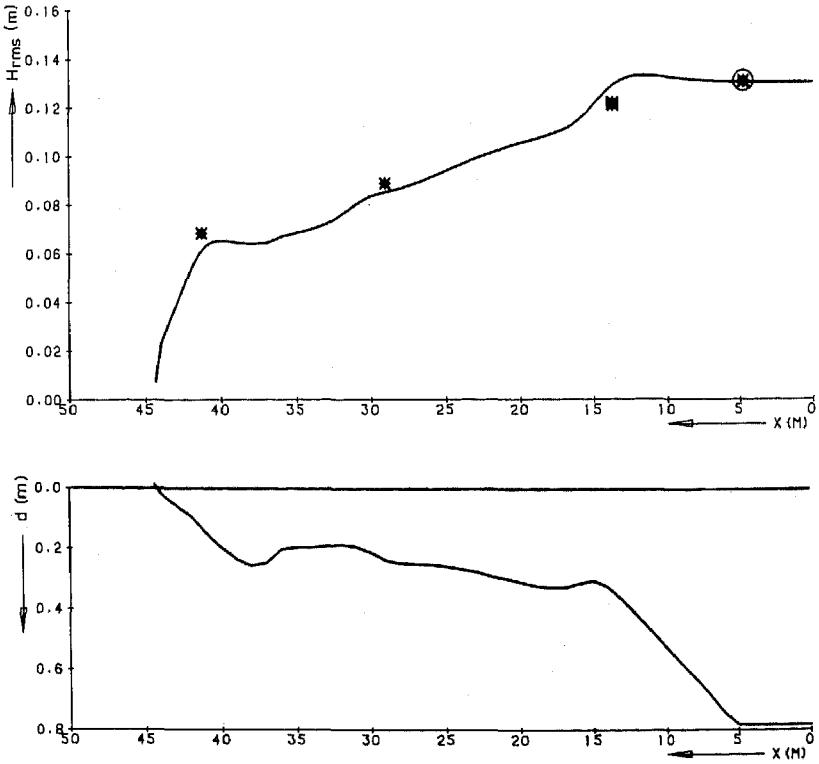

Fig. 5. Results for case 15 (laboratory). For legend, see Figure 3 (except $\bar{\eta}$).

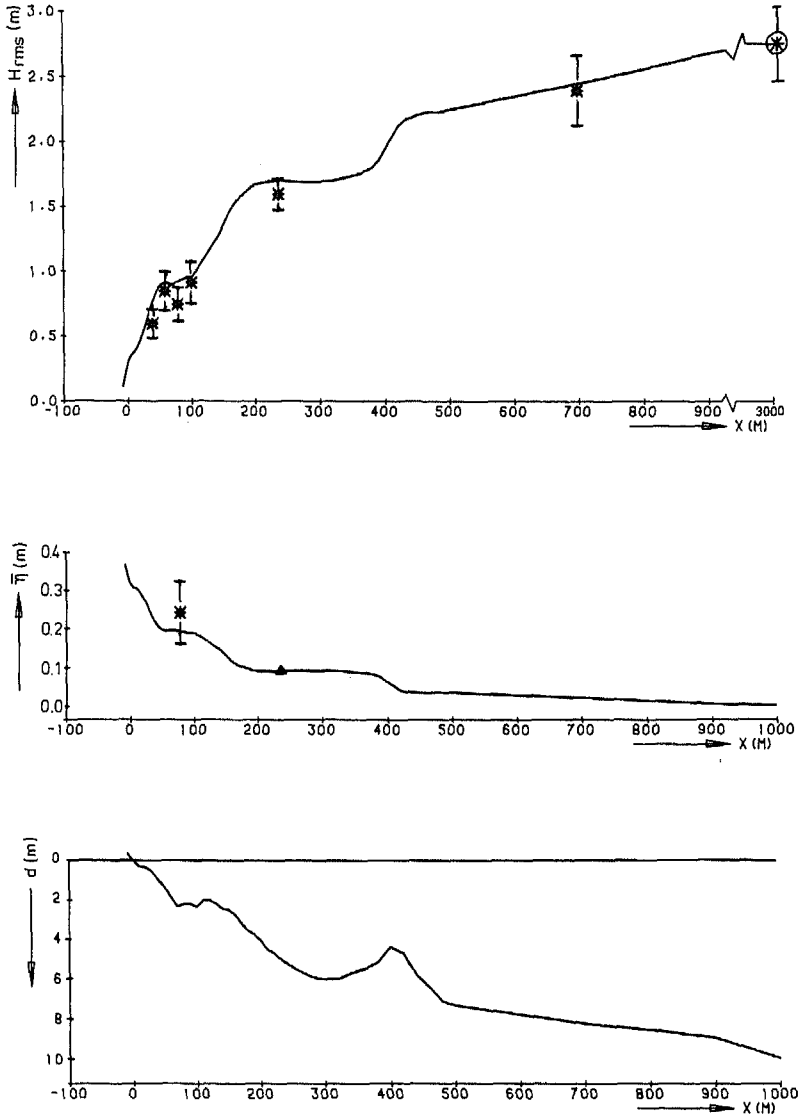

Fig. 6. Results for case 18 (field, Egmond beach). For legend, see Figure 3. The vertical line segments indicate one standard deviation on either side of the plotted data point.

other. However, in the calibration process just described there is a dependence between the two, since in this process the model is forced to simulate a certain energy dissipation, which depends on α and γ (through its proportionality to the product $\alpha Q H_m^2$; see (4)). Therefore there is effectively only one degree of freedom in tuning the model to a measured wave height variation. The calibration was in fact carried out by estimating optimal values of γ (denoted as $\hat{\gamma}$) under the constraint $\alpha = 1$. The resulting values of $\hat{\gamma}$ are listed in column 8 of Table 1. They fall in the range from 0.60 to 0.83, which is physically realistic. A graphical impression of the computed and measured H_{rms} variations is presented in a following section.

4.2. *Coefficient Parameterization*

It is known that the process of wave breaking in shallow water is influenced by the incident wave steepness and by the bottom profile, in particular, the slope. In some cases the influence of these two parameters is expressed sufficiently through a specific combination of wave steepness and bottom slope, the so-called surf similarity parameter [*Battjes*, 1974]. It was therefore investigated whether the estimated $\hat{\gamma}$ values vary systematically with these parameters. No significant variation of $\hat{\gamma}$ with beach slope separately or with the surf similarity parameter could be found. However, there did appear to be a slight but systematic dependence of $\hat{\gamma}$ on the deep-water steepness s_0, as can be seen in Figure 2. A hyperbolic tangent function has been fitted to these data, with the result

$$\hat{\gamma} = 0.5 + 0.4 \tanh (33 s_0) \tag{9}$$

This relation, indicated in Figure 2 by the solid line, can be used for purposes of prediction.

5. EVALUATION OF MODEL PERFORMANCE

In order to gain an impression of the overall performance of the model, we have applied it again to each of the 20 cases considered, this time using the parameterization (9) given above. Some examples of the results are shown in Figures 3–7. It can be seen that the model is quite realistic in the simulation of the observed rms waveheights. A comparison of normalized computed and measured H_{rms} values in the zone of wave shoaling and breaking covering all 20 cases is given in Figure 8. The correlation coefficient is 0.98; the model bias

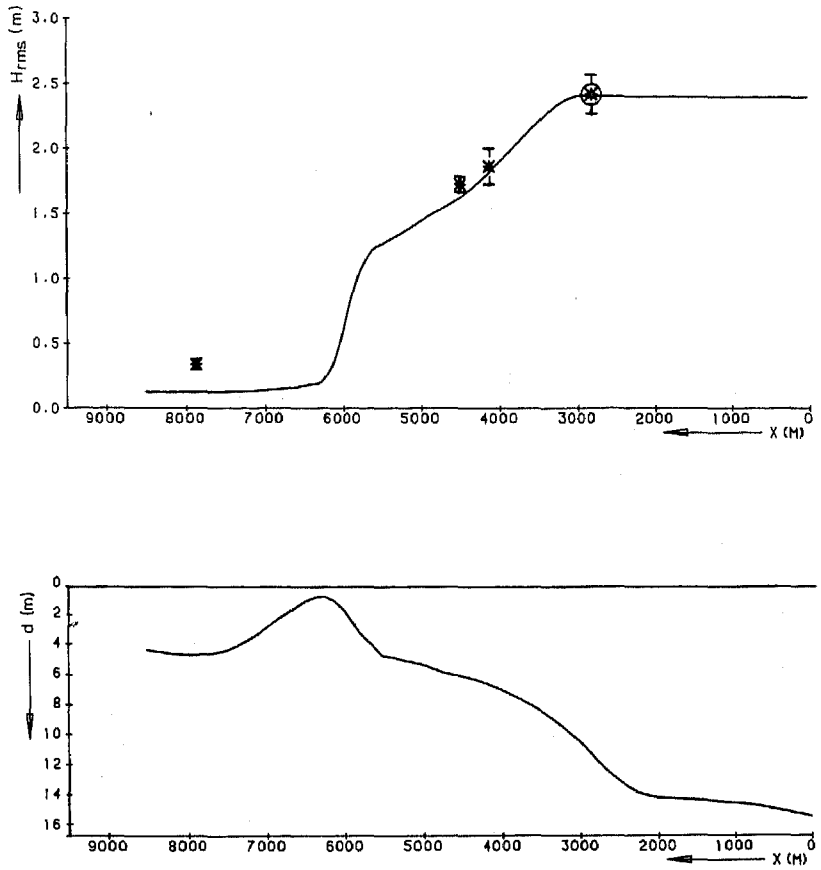

Fig. 7. Results for case 20 (field, Haringvliet shoal). For legend see Figure 6.

based on the best fitting proportional relationship is 0.01, and the rms relative error, normalized with the mean value of all measured values of H_{rms}/H_{rms_0} shown in Figure 8, is 0.06. These numbers confirm in a quantitative sense the high degree of realism possessed by the model for the prediction of the wave height variation in areas of wave breaking.

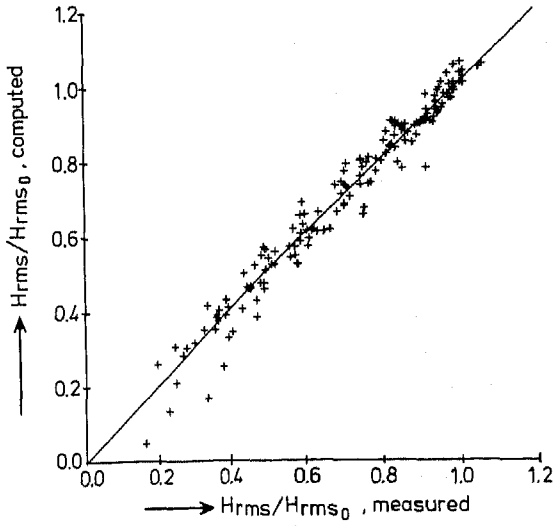

Fig. 8. Comparison of calculated and measured rms wave heights, normalized with the deep-water value. The calculated values are based on the parameterization given by (9). The straight line is the least squares, best fit proportional relationship.

The maximum setup also is well predicted (Figures 3 and 4), but in areas of large setup gradient the predicted rise is systematically too far seaward. This phenomenon has been noted previously by *Battjes* [1972] and by BJ. It suggests that the decrease in momentum flux lags behind the decrease in wave energy as measured through the variance of the surface elevation. A possible explanation for this phenomenon would be a relative surplus of kinetic energy in the area of intensive wave energy dissipation. This might consist partly of a surplus of kinetic wave energy (coherent with the surface elevation) and partly of turbulence energy. The latter possibility can be investigated by adding turbulent Reynolds stresses to the radiation stresses, e.g., on the basis of the model for turbulence in the surf zone presented by *Battjes* [1975]. However, this matter has not been pursued in the present study.

6. Discussion

The empirical evidence presented above indicates that the model predicts the rms wave height variation due to breaking very well in a wide range of conditions as far as bottom profile and incident waves are concerned. This is remarkable in view of the complexity of the physical processes involved, and the relatively simple concept on which the model is based. Moreover, in the elaboration of this concept, some simplifying approximations have been made.

One approximation used by BJ pertains to the estimation of the mean square of the heights of breaking waves. This mean square was approximated with the square of a characteristic height of breaking waves in the local depth, without considering the probability distribution of the heights of breaking waves in detail. The fraction of breaking waves at a given

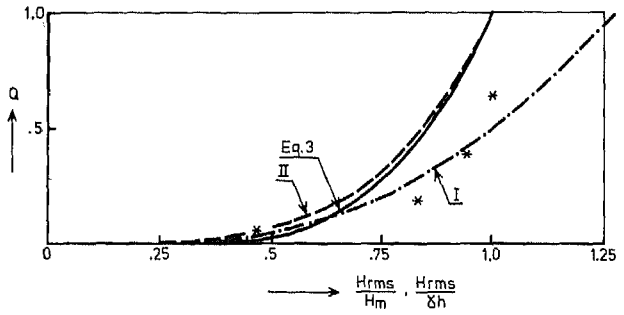

Fig. 9. Fraction of breaking waves (Q) versus relative rms wave height. Data points: *Thornton and Guza*'s [1983] measurements of Q versus $H_{rms}/(\gamma h)$ for $\gamma = 0.42$. curves I and II: *Thornton and Guza*'s [1983] approximation 1 and 2 to the data points. Curve labeled "eq. 3": *Battjes and Janssen*'s [1978] theoretical relation between Q and H_{rms}/H_m ((3) of this paper).

point was estimated on the same basis. These approximations appear to be sufficient for the estimation of the average wave energy dissipation.

Thornton and Guza [1983] have made field observations of the distribution of the heights of breaking waves on a beach. They have used the results to formulate a modification of BJ's model, which concerns the procedure of averaging over the breaking wave heights. To this end, they have used two empirically based analytical expressions for the probability density of the heights of breaking waves. One of these (their equations 11, 17 and 21 with $n = 2$), which here for brevity is called approximation 1, was obtained by curve fitting. The second one (based on their equation 20 instead of equation 21, here called approximation 2) did not fit nearly as well to the data; it was chosen to allow an analytical solution for the onshore wave height variation. However, the rms wave height variation predicted from the two schematizations was hardly different, provided the optimum value of a proportionality coefficient in the expression for the energy dissipation rate (comparable to α in this paper) was allowed to be different for the two approximations. This corresponds to the approach used above in the parameterization of the model coefficients α and γ, which were seen to be dependent if a certain dissipation is to be simulated. It also confirms the idea on which BJ's simpler approximation was based, namely that the details of the distribution of the breaking wave heights are not important for the estimation of the average energy dissipation.

Thornton and Guza's two approximations to the observed probability density functions of the heights of breaking waves contain γh as a scale parameter. Both approximations allow an analytical expression for the fraction of breaking waves (Q) as a function of $H_{rms}/(\gamma h)$. The results are shown in Figure 9. These can be compared with BJ's theoretical estimate given by (3), which is also shown in Figure 9. (For this comparison, H_m is set equal to γh.) It appears that Thornton and Guza's empirical formulation (2) gives approximately the same results for the fraction of breaking waves as BJ's theoretical expression.

Thornton and Guza's field data of Q versus $H_{rms}/(\gamma h)$ are also given in Figure 9. These are based on a value of $\gamma = 0.42$, obtained from an observed saturation value of H_{rms}/h in shallow water. The data lend support to the expectation that the fraction of breaking waves is a function of the ratio of H_{rms} to a typical breaker height.

The dissipation model used above is based on an assumed similarity betwen a breaking wave in shallow water and a bore. Detailed investigations of this assumption have been made by *Svendsen and Madsen* [1981] and *Stive* [1984*a*]. The results confirm the validity of this approach in order of magnitude. Stive finds a correction factor depending on the breaker type through the beach slope and the incident wave steepness. In this paper, we have used a constant value ($\alpha = 1$) in the parameterization; effects of deviations from this constant value are accounted for empirically in the breaker height coefficient γ. This means that the estimated optimal values of γ cannot directly be compared with observed ratios of breaking wave height to water depth. However, the deviations found by *Stive* [1984] are not so large as to invalidate the approach used in our parameterization. This is confirmed by the fact that the optimal values of $\hat{\gamma}$ are in a realistic range for breaker height coefficients (although the trend of its variation with wave steepness is opposite to that found from measurements of breaker height-to-depth ratio).

In the situations used in the calibration described herein, the wave propagation was one-dimensional, and without significant sources or sinks of energy between deep water and the surf zone. In applications, more complicated situations may arise, involving depth and/or current-induced refraction, energy input by wind, and energy dissipation in a bottom boundary layer. Although in such cases the energy balance becomes more complicated than the one used here, the expression for the rate of energy dissipation due to breaking (4) itself is unaffected; it is simply one sink in a set of other source/sink terms. Examples of the application of (4) in cases of two-dimensional propagation are given by *Dingemans et al.* [1984], who present additional empirical evidence confirming the validity of this approach.

7. Conclusions

A calibration is performed of a theoretical model for the wave energy dissipation and resulting wave energy variation in random breaking waves. Small-scale and large-scale (H_{rms} up to 1 m) laboratory data have been used, as well as field data. Bottom profiles were plane, concave, and barred. The incident wave steepness (based on H_{rms} and wavelength at the spectral peak) ranged from 0.01 to 0.04.

The theoretical model has effectively one adjustable parameter. Based on a comparison of calculated and measured variations of rms wave heights in areas of wave breaking, optimal values of this coefficient have been determined. These vary slightly in a physically realistic range with the incident wave steepness. A parameterization of this dependence is presented. Using this parameterization, the overall performance of the model has been evaluated. The coefficient of correlation between predicted and observed H_{rms} values is 0.98; the model bias is not significantly different from zero, and the rms relative error is 0.06. The maximum set up of the mean water level also is well predicted, although the predicted interval of steepest rise of the mean water level is systematically too far seaward. It is hypothesized that this is due to an underestimation of the total kinetic energy and momentum flux in areas of intense breaking, for a given potential energy of the wave.

In summary, the theoretical model presented by *Battjes and Janssen* [1978] for the prediction of the variation of wave energy and the associated radiation stresses in areas of wave breaking is found to perform very well for a wide range of conditions. It can be used with confidence for purposes of prediction, using a parameterization of its single adjustable coefficient in terms of wave steepness.

Acknowledgment. The authors wish to express their gratitude to H. Derks, M. W. Dingemans, and J. van Overeem, who supplied additional information on the measurement results obtained by them in their respective studies. Furthermore M. W. Dingemans is thanked for his support in developing the numerical model.

REFERENCES

Battjes, J. A., Set-up due to irregular waves, in *Proceedings of the 13th International Conference on Coastal Engineering*, pp. 1993–2004, American Society of Civil Engineers, New York, 1972.

Battjes, J. A., Surf similarity, in *Proceedings of the 14th International Conference on Coastal Engineering*, pp. 466–480, American Society of Civil Engineers, New York, 1974.

Battjes, J. A., A turbulence model for the surf zone, in *Proceedings, Symposium on Modelling Techniques*, pp. 1050–1061, American Society of Civil Engineers, New York, 1975.

Battjes, J. A., and J. P. F. M. Janssen, Energy loss and set-up due to breaking of random waves, in *Proceedings of the 16th International Conference on Coastal Engineering*, pp. 569–587, American Society of Civil Engineers, New York, 1978.

Collins, J. I., Probabilities of breaking wave characteristics, in *Proceedings of the 12th International Conference on Coastal Engineering*, pp. 399–412, American Society of Civil Engineers, New York, 1970.

Derks, H., and M. J. F. Stive, Field investigations in the TOW study programme for coastal sediment transport in The Netherlands, in *Proceedings of the 19th International Conference on Coastal Engineering*, pp. 1830–1845, American Society of Civil Engineers, New York, 1984.

Dingemans, M. W., Verification of numerical wave propagation models with field measurements; Crediz verification Haringvliet, *Rep. W 488*, Delft Hydraul. Lab., The Netherlands, 1983.

Dingemans, M. W., M. J. F. Stive, A. J. Kuik, A. C. Radder, and N. Booij, Field and laboratory verification of the wave propagation model Crediz, in *Proceedings of the 19th International Conference on Coastal Engineering*, pp. 1178–1191, American Society of Civil Engineers, New York, 1984.

Goda, Y., Irregular wave deformation in the surf zone, *Coastal Eng. Jpn.*, *18*, 13–26, 1975.

LeMéhauté, B., On non-saturated breakers and the wave run-up, in *Proceedings of the 8th International Conference on Coastal Engineering*, pp. 77–92, American Society of Civil Engineers, New York, 1962.

Longuet-Higgins, M. S., and R. W. Stewart, A note on wave set-up, *J. Mar. Res.*, *75*, 4–10, 1963.

Stive, M. J. F., Energy dissipation in waves breaking on gentle slopes, *J. Coastal Eng.*, *8*, 99–127, 1984.

Stive, M. J. F., A scale comparison of waves breaking on a beach, *J. Coastal Eng.*, *9*(2), 151–158, 1985.

Stoker, J. J., *Water Waves*, Interscience, New York, 1957.

Svendsen, I. A., and P. A. Madsen, Energy dissipation in hydraulic jumps and breaking waves, *Progr. Rep. 55*, pp. 39–47, Inst. Hydrodyn. Hydraul. Eng., Tech. Univ. Denmark, 1981.

Thornton, E. B., and R. T. Guza, Transformation of wave height distribution, *J. Geophys. Res.*, *88*, 5925–5938, 1983.

Van Overeem, J., Morphologic behaviour of beach fill with underwater dam, *Rep. M 189 I*, Delft Hydraul. Lab., The Netherlands, 1983.

J. A. Battjes, Delft University of Technology, Department of Civil Engineering, P. O. Box 5048, 2600 GA Delft, The Netherlands.

M. J. F. Stive, Delft Hydraulics Laboratory, The Netherlands.

(Received August 30, 1984;
accepted February 11, 1985.)